Energy & Environmental Science

COMMUNICATION

View Article Online
View Journal | View Issue

Cite this: *Energy Environ. Sci.*, 2016, **9**, 141

Received 3rd December 2015,
Accepted 11th December 2015

DOI: 10.1039/c5ee03649f

www.rsc.org/ees

Transition metal carbides as novel materials for CO_2 capture, storage, and activation†

Christian Kunkel, Francesc Viñes and Francesc Illas*

The capture and activation of the greenhouse gas carbon dioxide (CO_2) is a prerequisite to its catalytic reforming or breakdown. Here we report, by means of density functional theory calculations including dispersive forces, that transition metal carbides (TMC; TM = Ti, Zr, Hf, Nb, Ta, Mo) are able to uptake and activate CO_2 on their most-stable (001) surfaces with considerable adsorption strength. Estimations of adsorption and desorption rates predict a capture of CO_2 at ambient temperature and even low partial pressures, suggesting TMCs as potential materials for CO_2 abatement.

Carbon dioxide (CO_2) is an active greenhouse gas with a rising atmospheric concentration currently approaching a value of 400 ppm. This raises concerns about serious consequences such as climate change and ocean acidification.[1] As economies and energy demand are projected to grow in the future,[2] a reduction of CO_2 emissions nowadays only seems possible with efficient technologies for carbon capture and storage (CCS),[3–6] employing absorbents or solvents.[7] CO_2 re-use into a saleable product has been suggested to be an appealing route to contribute to climate change mitigation, though the field is still in its infancy and questions over overall system efficiency have been raised.[7–9] Active catalytic systems for such processes are known, yet most of them are made of scarce and precious metals, normally supported on high surface area porous oxides or sulfides.[10,11] The effective large-scale implementation on this basis then still remains a great challenge.[11–13]

In the search for new active catalysts, numerous endeavours address the adsorption, activation, and subsequent catalytic conversion of CO_2 on different systems. Note that a relatively high adsorption energy is needed for CO_2 to stick on a catalyst surface, which is made difficult by the high stability of CO_2 molecules. Moreover, when possible, CO_2 adsorption normally goes without significant activation, a process that is known to require charge transfer from the substrate resulting in a concomitant bending.[14] The possible capture/activation of CO_2 has been theoretically tackled *via* first principles calculations on metals,[15–17] metal oxides,[18,19] graphene-based materials,[20] sulfides,[21] zeolites,[22] and metal–organic frameworks,[23] to name a few.

Since the surface chemistry of transition metal carbides (TMCs) was described as comparable to that of Pt-group metals by Levy and Boudart,[24,25] these materials have received considerable attention in catalysis. TMC based catalysts have been used in a wide range of reactions like methane dry reforming,[26] conversion of methane to synthesis gas,[27] desulfurization,[28] hydrogenation,[29] the water-gas-shift reaction,[30] and CO oxidation,[31] demonstrating chemical robustness and oftentimes catalytic properties similar to precious Pt-group metals.

The interaction of CO_2 and TMC surfaces has been recently reviewed,[10,32] although one must acknowledge that most of the studies so far focused on Mo_2C, MoC, WC, and TiC. From these studies it is now known that some surfaces of Mo_2C, δ-MoC, and TiC are highly active for CO_2 hydrogenation, producing methanol, methane, and carbon monoxide (CO) in different ratios.[33–35] The catalytic activity of these TMCs has been found to be further enhanced by using them as supports for transition metal nanoclusters.[34,36] Regarding CO_2 adsorption and activation, density functional theory (DFT) calculations have shown that upon interaction with these surfaces a surface-bound anionic $CO_2^{\delta-}$ species with bended geometry is formed. Many CO_2 surface chemistry studies[37,38] evidence the key role of this activated intermediate in further reactions.

Apart from the above-mentioned extensively studied systems, information on the CO_2 surface chemistry involving other TMCs is rather limited. A recent study carried out by Porosoff and coworkers[35] found CO_2 hydrogenation activities for TiC, ZrC, NbC, TaC, WC, and Mo_2C. These results largely motivated the present theoretical systematic investigation of CO_2 adsorption and activation on TMC surfaces. To facilitate a logical comparison of the results and to circumvent structural aspects and related effects, we restrained our study to TMCs with a 1:1

Departament de Química Física & Institut de Química Teòrica i Computacional (IQTCUB), Universitat de Barcelona, c/Martí i Franqués 1, 08028 Barcelona, Spain. E-mail: francesc.illas@ub.edu

† Electronic supplementary information (ESI) available: Computational details, list of adsorption energies and geometric descriptors, top views of adsorbate structures, brief explanation of the used rate model. See DOI: 10.1039/c5ee03649f

TM : C ratio and a face-centered cubic (fcc) crystallographic structure and, among possible surfaces, we chose the (001) one, known to be most stable one for fcc TMCs.[39] In particular, we studied TiC, ZrC, and HfC (group 4), VC, NbC, and TaC (group 5), and δ-MoC (group 6). Note that for MoC fcc packing is only present in the high temperature δ-phase.

Periodic DFT calculations aimed at studying the interaction of CO_2 with the TMC(001) surfaces have been carried out within the generalized gradient approximation (GGA) using the Vienna *Ab-Initio* Simulation Package – VASP 5.3.5 code.[40] In order to account for exchange correlation effects the Perdew–Burke–Ernzerhof (PBE) exchange–correlation functional was used,[41] alone or adding the D3 dispersion correction (PBE-D3) developed by Grimme.[42] Further computational details are given in the ESI.† For a better understanding of the oncoming discussion it is worth to restate that favourable adsorption energies, E_{ads}, are defined negative, and that interactions are more favourable for lower values of E_{ads}.

In a first step sites that might strongly bind and activate CO_2 have been identified. There are MCC, MMC, TopM, and TopC sites as defined by Posada-Pérez *et al.*[33] and all were explicitly considered for CO_2 on TiC, VC, and δ-MoC(001) surfaces, thus including cases from group 4 to group 6. In no case E_{ads} values smaller than −0.05 eV were found on the VC(001) surface, and therefore this carbide has been excluded from further discussion. The tested MCC and TopM sites yielded non-activated physisorbed situations, although on δ-MoC(001) with sensible adsorption energies around −0.5 eV.

Regardless of the previous, the adsorption energies on MMC and TopC sites are significantly high, −0.89 and −0.71 eV on δ-MoC(001), and −0.55 and −0.57 eV on TiC(001), as obtained at the PBE level, comparing well with the previously reported values[33,43] and comparable to the most favourable cases involving metal surfaces. For instance, for CO_2 on Ni(110), Co(110), and Fe(100) E_{ads} values of −0.39 eV, −0.61 eV, and −0.72 eV, respectively, have been reported at the GGA level.[15–17] Note, however, that these E_{ads} values are obtained for the most open and, consequently, least stable and most reactive low Miller indices surfaces, at variance with current TMCs, where CO_2 is studied on the most stable surface.

Having identified MMC and TopC sites as the most active ones for δ-MoC and TiC we further explored these sites in the rest of TMC(001) surfaces. In order to also investigate the role of dispersive (van der Waals) forces, we contemplated the study also at the PBE-D3 level. In all cases we found a favourable adsorption of CO_2, see PBE-D3 E_{ads} values in Table 1; for PBE values we refer to the ESI.† Note from these values that the competition among MMC and TopC sites is especially acute for group 4 TMCs, where the adsorption energy difference $\Delta E_{ads} = E_{ads}(MMC) - E_{ads}(TopC)$ is at most of 0.04 eV. The difference becomes larger for NbC and δ-MoC(001) surfaces, with ΔE_{ads} = −0.17 eV, and reaches a maximum for TaC, where ΔE_{ads} = −0.27 eV. It should be mentioned that ΔE_{ads} are equal within 0.01 eV for both PBE and PBE-D3 methods.

From the tabulated values, trends for adsorption energies can be withdrawn. For instance, on 3*d*, 4*d*, and 5*d* TMC(001) E_{ads} rise in magnitude when going down a group. Aside, the adsorption strength decreases when moving along a *d* series. Indeed, the almost vanishing interaction of CO_2 on the VC(001) surface can be understood from the decrease of more than 0.7 eV when going ZrC → NbC, applying the same trend in going from TiC to VC would result in an E_{ads} value of at most 0.1 eV at the PBE level, in full concordance with the obtained results. One must warn, however, that these trends may not hold for other stable surfaces, as the surface structure can strongly alter the adsorptive properties.[15,17]

Last but not the least, it is mandatory to highlight that, compared to PBE E_{ads} values, PBE-D3 predicts more stable minima by 0.21–0.32 eV. Still, the main adsorption driving force comes from non-dispersive interactions between the surface and the adsorbate, as already found for other TMCs as well.[10] In the δ-MoC(001) surface a fair comparison between D3 and D2 dispersion corrections reveals that, compared to PBE,[33] the latter yields a slightly larger stabilization (0.4–0.6 eV).

Note that on both MMC and TopC sites, and regardless of the TMC, the adsorbed CO_2 molecule exhibits a similar geometry, see examples of the adsorbate structures on the TiC(001) surface in Fig. 1. For each system, a complete list of structural descriptors, including bond lengths and molecular angles, is reported in Table S1 of the ESI.† Briefly, and in agreement with earlier results, C ↔ C and metal ↔ O interactions between CO_2 and surface site atoms imply bond lengths on the order of 1.46–1.50 and 2.09–2.37 Å, respectively. Compared to MMC sites, the latter are *circa* 0.2 Å longer on TopC. The adsorbed CO_2 species always bend with angles α(OCO) between 120.1 and 128.8° which is a strong evidence of CO_2 activation by charge transfer from the underlying TMC surface.[10]

This is also consistent with C–O bond lengths between 1.29 and 1.32 Å, significantly longer than the 1.176 Å value of CO_2 in a vacuum.

Given the relatively high adsorption energies, there is a clear interest in estimating the temperature fringe below which these

Table 1 Adsorption energies, E_{ads}, and differences, ΔE_{ads}, of CO_2 and TopC sites of different TMC(001) surfaces. All values are given in eV

E_{ads}	TiC	ZrC	HfC	NbC	TaC	δ-MoC
MMC	−0.81	−1.56	−1.62	−0.87	−1.21	−1.20
TopC	−0.83	−1.60	−1.65	−0.70	−0.94	−1.03
ΔE_{ads}	0.02	0.04	0.03	−0.17	−0.27	−0.17

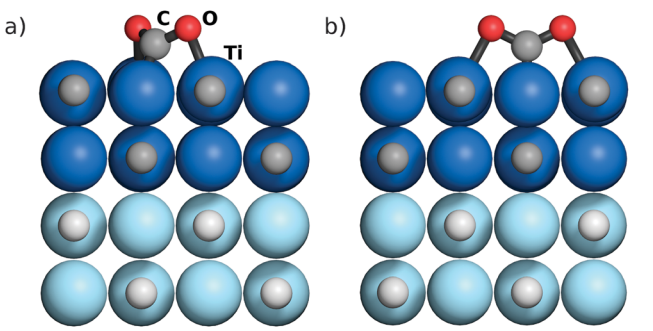

Fig. 1 Side sketches of CO_2 adsorbed on (a) MMC and (b) TopC sites of the TiC(001) surface. Atom labels indicate the sphere colouring. Lighter colour layers were fixed during optimization. For respective top views see Fig. S1 of the ESI.†

TMCs could capture and accumulate CO_2. This can be easily assessed from adsorption and desorption rates, r_{ads} and r_{des}, respectively, which can be estimated in the framework of the transition state theory (TST). Hence, r_{ads} and r_{des} values have been calculated over a temperature range up to 1000 K with necessary quantities obtained from the above commented DFT calculations. The utilized equations and approaches are duly explained in the ESI.† In a nutshell, the adsorption rate depends on the impingement of CO_2 to the surface and therefore, on the CO_2 partial pressure (p_{CO_2}). In this sense, and for each system, r_{ads} has been calculated for (i) the current atmospheric partial pressure of CO_2, p_{CO_2} = 40 Pa,[44] (ii) for p_{CO_2} = 15 000 Pa—0.15 bar—, a benchmark value for postcombustion exhaust gases,[5] and (iii) p_{CO_2} = 10^5 Pa—1 bar—a partial pressure regime of interest for pure CO_2 stream generation from a CCS system.[7]

The desorption rates largely depend on the adsorption strength, and so we obtained four curves for each TMC, two for MMC and two for TopC sites, each of them as evaluated using PBE or PBE-D3 calculations respectively. DFT calculations are widespread used for evaluating adsorption strengths on a plethora of substrates, whilst TST is frequently used for simulating desorption processes as in temperature programmed desorption; a recent study for CO adsorption/desorption on a similar system (TiC nanopowders) provides a paradigmatic example.[45]

The estimated r_{ads} and r_{des} rates are graphically shown for the two fringe cases TiC and ZrC, see Fig. 2a. These are representative TMCs with low and high E_{ads} values. Note that intersection points of r_{ads} and r_{des} define temperatures below which adsorption prevails and, consequently, CO_2 accumulates on the TMC surface. Thus, for TiC(001) at 40 Pa CO_2 partial pressure, the lowest and highest intersection temperatures are 211 K for the MMC site as calculated using PBE and 329 K for the TopC site (PBE-D3), marked as T_1 and T_2, respectively. At a CO_2 partial pressure of 0.15 bar the intersection temperatures are shifted to higher values of 262 to 414 K (T_3 and T_4), and so compare to the desorption temperature of 323 K reported for the zeolite 13X benchmark material.[5] At a CO_2 partial pressure of 1 bar, the desorption process will likely occur in the 285–452 K range (T_5 and T_6), temperatures above which a surface regenerate for further use becomes feasible.

Thus $T_1 \rightarrow T_2$, $T_3 \rightarrow T_4$, and $T_5 \rightarrow T_6$ can be interpreted as temperature ranges in which the TMC(001) surface looses its ability to initially capture and accumulate CO_2 when annealing. This seems reasonable as dispersive force contributions to the adsorption energies might be overestimated by PBE-D3 and we expect the real desorption rate to lie somewhere in between. The analysis for the rest of investigated TMCs is summarized in Fig. 2b allowing for an easy comparison. Thus, ZrC- and HfC(001) surfaces display very elevated temperature ranges, in accordance with their high adsorption energies. The temperature ranges for TiC, NbC, TaC, and δ-MoC are lower but still in the range or even well above room temperature. Even though no CCS experiments on TMCs are available, it has been experimentally proven, as mentioned above, that some TMCs catalyse the CO_2 hydrogenation to methanol at 500–600 K,[33–35] implying that CO_2 must become an adsorbed surface activated moiety.

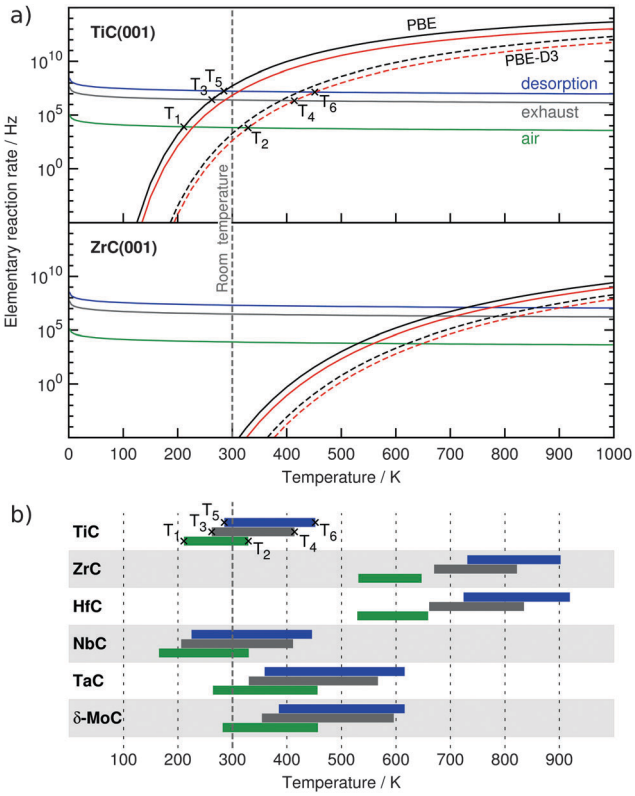

Fig. 2 (a) Calculated rates for desorption and adsorption of CO_2 on TiC and ZrC(001) surfaces. On TiC, marked points with T_1–T_6 labels in (a) and (b) show how desorption temperature ranges in (b) have been obtained. Legend for (a): green, grey, and blue; adsorption rates on a single site per time unit for a CO_2 partial pressure of 40, 15 × 10^3, and 10^5 Pa, respectively. Black and red; desorption rates per site and time unit from MMC and TopC sites. PBE (solid) and PBE-D3 (dashed) values are provided. Legend for (b): green, grey, and blue bars belong to desorption temperature ranges for CO_2 partial pressures of 40, 15 × 10^3, and 10^5 Pa, respectively.

Note that, as stated above, in most of these cases, MMC sites show a stronger adsorption compared to TopC sites, with a concomitant widening of the calculated temperature range. One must keep in mind that upon annealing, these systems may well first partially lose their adsorption capability, *i.e.* those TopC sites would be firstly depopulated, yet here lateral interactions are being neglected, and so the obtained rates better correlate with the initial stages of CO_2 capture. Nevertheless, at low coverages on Ni surfaces,[17] lateral interactions for adsorbed CO_2 have been found not to be repulsive and so initial desorption rates are likely not underestimated. All in all, most of the TMC(001) surfaces are envisaged to capture and accumulate CO_2 at ambient and even elevated temperatures.

In summary, periodic DFT calculations carried out at the PBE level and also including dispersion (PBE-D3) showed that CO_2 molecules adsorb and get activated on a range of stable (001) surfaces of transition metal carbides (TMC–TM = Ti, Zr, Hf, Nb, Ta, Mo). Two competitive adsorption sites are identified (MMC and TopC) where CO_2 chemisorbs in a bended (activated) geometry. Dispersion corrected adsorption energies are found to be favourable and lie in a range of −0.70 to −1.65 eV, depending

on the TMC and surface site. These adsorption strengths are therefore considerably high, and despite dispersive forces are responsible of 0.21–0.32 eV, the major attachment force has a chemical nature. Adsorption and desorption rates, as predicted from DFT data, show that these materials theoretically can adsorb CO_2 up to elevated temperatures at even low partial pressures. Thus TMCs appear to be ideal materials for CO_2 capture and abatement, and actually given its activated adsorption appealing for using them as catalysts for CO_2 conversion as well.

This work was supported by Spanish *Ministerio* grants (CTQ2012-30751) and *Generalitat de Catalunya* grants (2014SGR97 and XRQTC). F. V. thanks the Spanish *Ministerio de Economía y Competitividad* for the *Ramón y Cajal* postdoctoral grant (RYC-2012-10129).

Notes and references

1 Intergovernmental Panel on Climate Change, *Climate Change 2013 – The Physical Science Basis*, Cambridge University Press, 1st edn, 2014.
2 International Energy Agency, *World Energy Outlook 2014*, Paris, 2014.
3 A. Sayari, Y. Belmabkhout and R. Serna-Guerrero, *Chem. Eng. J.*, 2011, **171**, 760.
4 L. Espinal, D. L. Poster, W. Wong-Ng, A. J. Allen and M. L. Green, *Environ. Sci. Technol.*, 2013, **47**, 11960.
5 D. M. D'Alessandro, B. Smit and J. R. Long, *Angew. Chem., Int. Ed.*, 2010, **49**, 6058.
6 S. Choi, J. H. Drese and C. W. Jones, *ChemSusChem*, 2009, **2**, 796.
7 M. E. Boot-Handford, J. C. Abanades, E. J. Anthony, M. J. Blunt, S. Brandani, N. Mac Dowell, J. R. Fernández, M.-C. Ferrari, R. Gross, J. P. Hallett, R. S. Haszeldine, P. Heptonstall, A. Lyngfelt, Z. Makuch, E. Mangano, R. T. J. Porter, M. Pourkashanian, G. T. Rochelle, N. Shah, J. G. Yao and P. S. Fennell, *Energy Environ. Sci.*, 2014, **7**, 130.
8 M. Aresta and A. Dibenedetto, *Dalton Trans.*, 2007, 2975.
9 G. Centi and S. Perathoner, *Top. Catal.*, 2009, **52**, 948.
10 S. Posada-Pérez, F. Viñes, J. Rodriguez and F. Illas, *Top. Catal.*, 2015, **58**, 159.
11 E. V. Kondratenko, G. Mul, J. Baltrusaitis, G. O. Larrazabal and J. Perez-Ramirez, *Energy Environ. Sci.*, 2013, **6**, 3112.
12 V. Havran, M. P. Duduković and C. S. Lo, *Ind. Eng. Chem. Res.*, 2011, **50**, 7089.
13 A. Otto, T. Grube, S. Schiebahn and D. Stolten, *Energy Environ. Sci.*, 2015, **8**, 3283.
14 F. Viñes, A. Borodin, O. Höfft, V. Kempter and F. Illas, *Phys. Chem. Chem. Phys.*, 2005, **7**, 3866.
15 V. A. de la Peña O'Shea, S. González, F. Illas and J. L. G. Fierro, *Chem. Phys. Lett.*, 2008, **454**, 262.
16 V.-A. Glezakou, L. X. Dang and B. P. McGrail, *J. Phys. Chem. C*, 2009, **113**, 3691.
17 S.-G. Wang, D.-B. Cao, Y.-W. Li, J. Wang and H. Jiao, *J. Phys. Chem. B*, 2005, **109**, 18956.
18 D. C. Sorescu, J. Lee, W. A. Al-Saidi and K. D. Jordan, *J. Chem. Phys.*, 2011, **134**, 104707.
19 Q.-L. Tang and Q.-H. Luo, *J. Phys. Chem. C*, 2013, **117**, 22954.
20 Y. Jiao, A. Du, Z. Zhu, V. Rudolph, G. Q. Lu and S. C. Smith, *Catal. Today*, 2011, **175**, 271.
21 N. Y. Dzade, A. Roldan and N. H. de Leeuw, *J. Chem. Phys.*, 2015, **143**, 094703.
22 D. Smykowski, B. Szyja and J. Szczygieł, *J. Mol. Graphics Modell.*, 2013, **41**, 89.
23 L. Valenzano, B. Civalleri, S. Chavan, G. T. Palomino, C. O. Areán and S. Bordiga, *J. Phys. Chem. C*, 2010, **114**, 11185.
24 H. H. Hwu and J. G. Chen, *Chem. Rev.*, 2005, **105**, 185.
25 R. B. Levy and M. Boudart, *Science*, 1973, **181**, 547.
26 A. Brungs, A. E. York and M. H. Green, *Catal. Lett.*, 1999, **57**, 65.
27 J. B. Claridge, A. P. E. York, A. J. Brungs, C. Marquez-Alvarez, J. Sloan, S. C. Tsang and M. L. H. Green, *J. Catal.*, 1998, **180**, 85.
28 J. A. Rodriguez, P. Liu, J. Dvorak, T. Jirsak, J. Gomes, Y. Takahashi and K. Nakamura, *Surf. Sci.*, 2003, **543**, L675.
29 P. M. Patterson, T. K. Das and B. H. Davis, *Appl. Catal., A*, 2003, **251**, 449.
30 F. Viñes, J. A. Rodriguez, P. Liu and F. Illas, *J. Catal.*, 2008, **260**, 103.
31 L. Ono and B. Roldán-Cuenya, *Catal. Lett.*, 2007, **113**, 86.
32 J. A. Rodriguez, P. Liu, D. J. Stacchiola, S. D. Senanayake, M. G. White and J. G. Chen, *ACS Catal.*, 2015, **5**, 6696.
33 S. Posada-Pérez, F. Viñes, P. J. Ramirez, A. B. Vidal, J. A. Rodriguez and F. Illas, *Phys. Chem. Chem. Phys.*, 2014, **16**, 14912.
34 M. D. Porosoff, X. Yang, J. A. Boscoboinik and J. G. Chen, *Angew. Chem.*, 2014, **126**, 6823.
35 M. D. Porosoff, S. Kattel, W. Li, P. Liu and J. G. Chen, *Chem. Commun.*, 2015, **51**, 6988.
36 J. A. Rodriguez, J. Evans, L. Feria, A. B. Vidal, P. Liu, K. Nakamura and F. Illas, *J. Catal.*, 2013, **307**, 162.
37 U. Burghaus, *Prog. Surf. Sci.*, 2014, **89**, 161.
38 H. J. Freund and M. W. Roberts, *Surf. Sci. Rep.*, 1996, **25**, 225.
39 F. Viñes, C. Sousa, P. Liu, J. A. Rodriguez and F. Illas, *J. Chem. Phys.*, 2005, **122**, 174709.
40 G. Kresse and J. Furthmüller, *Phys. Rev. B: Condens. Matter Mater. Phys.*, 1996, **54**, 11169.
41 J. P. Perdew, K. Burke and M. Ernzerhof, *Phys. Rev. Lett.*, 1996, **77**, 3865.
42 S. Grimme, S. Ehrlich and L. Goerigk, *J. Comput. Chem.*, 2011, **32**, 1456.
43 A. B. Vidal, L. Feria, J. Evans, Y. Takahashi, P. Liu, K. Nakamura, F. Illas and J. A. Rodriguez, *J. Phys. Chem. Lett.*, 2012, **3**, 2275.
44 T. Takahashi, S. Sutherland and A. Kozyr, *Global Ocean Surface Water Partial Pressure of CO_2 Database: Measurements Performed During 1957–2014 (Version 2014),* Environmental Sciences Division, Oak Ridge National Laboratory, 2015.
45 B. P. Mant, G. G. Asara, J. A. Anderson, N. Homs, P. Ramírez de la Piscina, S. Rodríguez, J. M. Ricart and F. Illas, *Surf. Sci.*, 2013, **613**, 63.

